

# FULLY AUTOMATIC 3D SEGMENTATION OF CORONARY ARTERIES BASED ON MATHEMATICAL MORPHOLOGY

B. Bouraoui<sup>1,2</sup>, C. Ronse<sup>1</sup>

J. Baruthio<sup>2</sup>, N. Passat<sup>1</sup>

Ph. Germain<sup>3</sup>

1. LSIIT, UMR ULP-CNRS 7005  
Strasbourg, France

2. LINC, UMR ULP-CNRS 7191  
Strasbourg, France

3. Service Radiologie,  
CHU Strasbourg, France

## ABSTRACT

In this paper we propose a fully automatic algorithm for coronary artery extraction from X-ray data (3D-CT scan, 64 detectors) based on the mathematical morphology techniques and guided by anatomical knowledge. Growing and thresholding methods, in their most general form, are not sufficient to extract only the whole coronary arteries, because of the properties of these images. Finding appropriate methods is known to be a challenging problem because of the data imperfections such as noise, heterogeneous intensity and contrasts of similar tissues. We deal with these challenges by employing discrete geometric tools to fit on the arteries form independently from any perturbation of the data.

**Index Terms**— coronary arteries, segmentation, anatomical knowledge, hit-or-miss transform, region-growing.

## 1. INTRODUCTION

Coronary artery diseases are the most common type of heart disease. They are generally the consequence of atherosclerosis which results in hardening and narrowing of arteries supplying blood to the heart muscle [1]. For diagnosis and treatment of such pathologies, three dimensional (3D) coronary arteries visualisation is highly suitable. 3D reconstruction (*i.e.* segmentation and 3D surfacic visualisation) of the coronary arteries from angiograms would lead to higher accuracy and reproducibility in the diagnosis and to better precision in the quantification of the severity of the diseases [2].

Segmentation strategies vary depending on the imaging modality, application domain, automation requirements, and other specific factors [3, 4]. Most of image processing concepts have been involved in such segmentation methods development. Among them, mathematical morphology is one of the most recently considered [5].

In this paper we propose a fully automatic method of segmentation of the coronary arteries in large X-ray images (which may be noisy and present variable contrasts between the different acquisitions [6]). To reach this goal, two methodologies are combined: the gray-level hit-or-miss transform and region-growing. The segmentation is performed in two steps. In the first one, we detect the artery which generates

the coronary arteries: the aorta, by application of a gray scale hit-or-miss transform followed by a region-growing. In the second one, detection of coronary arteries is performed using a hit-or-miss based region-growing initialised from seeds obtained in the first step. The paper is organised as follows. In section 2, background notions related to mathematical morphology, coronary arteries anatomy and X-ray images are introduced. In section 3, the segmentation method is fully described. Section 4 proposes experimental results. Finally, conclusion and further works are discussed in section 5.

## 2. BACKGROUND

### 2.1. Region-growing

Basically, region-growing methods are based on two main concepts: seed-point(s) and expansion criterion. Starting from the seed-point(s), and iteratively exploring - until stability - the currently segmented object neighborhood, if the expansion criterion is satisfied for a given point, this point is added to the object. With the data we are interested in, it can be assumed that vessels are brighter than the surrounding tissues, but a simple thresholding is not sufficient to define an expansion criterion because of two reasons: 1) the blood in heart cavities that are close to the arteries, in which a region-growing process can easily deflect, 2) the intensity and contrast variability of images from one acquisition to another, caused by the use of injected contrast agent. To obtain satisfying results in an automatic fashion, despite of these constraints, two requirements are essential [7]:

- no user seed-point selection but an automatically detected one;
- an expansion criterion independent of the variation of image properties.

### 2.2. Hit-or-miss transform

#### 2.2.1. Binary hit-or-miss transform

The hit-or-miss (HMT) in binary images is a classic mathematical morphology operator [8], that uses two structuring elements  $A$  and  $B$ . The operation is made by testing two conditions:  $A$  has to belong to the object, while  $B$  has to belong to the background. More formally, the HMT transform by the pair  $(A, B)$  associates to a binary image  $X$  the set  $X \otimes (A, B)$  of positions where the translate of  $A$  fits inside  $X$  and at the

bouraoui@lsiit.u-strasbg.fr

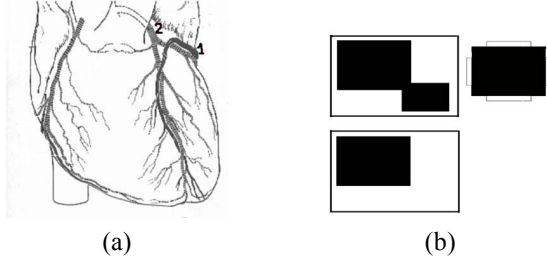


**Fig. 1.** (a) Heart anatomy: 1: coronary vein and 2: coronary artery, (b) Binary HMT: above to the left: original image, above to the right: structuring element and down: result of the binary HMT.

same time the translate of  $B$  fits inside the complement  $X^c$  of  $X$ : An example of binary HMT is illustrated in Fig. 1(b).

### 2.2.2. Gray-level hit-or-miss transform

The binary HMT operator is not easily extended to gray-level images. We use a definition of HMT operator [9] that assigns to  $A$  and  $B$  gray-levels  $a$  and  $b$ , respectively. Following this definition, the gray-level (GL) HMT compares the minimum intensity  $a_{min}$  in  $A$  to the maximum intensity  $b_{max}$  in  $B$ :

$$S_s^t = I_s \otimes (A, B)(p) = \begin{cases} (I_s \ominus A)(p) - a & \text{if } (I_s \ominus A)(p) \geq (I_s \oplus B)(p) + a - b \neq +\infty \\ -\infty & \text{otherwise} \end{cases} \quad (1)$$

If  $a_{min} > (b_{max} + a - b)$ , then the point is selected by the GL HMT. An example of HMT is illustrated in Fig. 2.

The GL HMT is devoted to the detection of patterns which can be discriminated by their shape (*i.e.* their geometrical properties), the shape of their background, and the intensity difference between them.

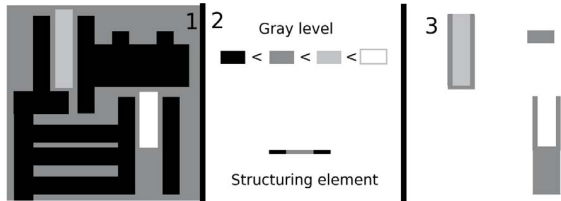


**Fig. 2.** Gray-level HMT application, 1: Original image, 2: Structuring element, 3: Result of the GL HMT.

### 2.3. X-ray data and coronary artery anatomy

The images which are supposed to be processed by the developed method are 3D X-ray data visualising the heart region, and especially the vascular structures, thanks to injection of a contrast agent. These images have a submillimetric resolution ( $0.6 \times 0.6 \times 0.6$  to  $1.2$  mm), resulting in a large size ( $512^3$ ), and are generally anisotropic on the axial dimension. In addition to the heart, these images visualise a large part of the

trunk, including the lungs, the spinal column, the liver and a part of the stomach (Fig. 3(a)).

The coronary arteries, which have to be segmented from these images, are composed of two vessels (the left coronary artery and the right one). Both of them originate from the beginning of the aorta, immediately above the aortic valve (Fig. 1(a)). The aorta is the largest single blood vessel in the body, corresponding to a large tubular structure whose axial section is circular at almost 3 cm from the aortic valve and presenting a wall sufficiently thick to be visualized in the data.

## 3. SEGMENTATION METHOD

### 3.1. Input/output

The method requires as input a 3D X-ray image  $I$  of the heart similar to those presented previously. Such an image can be considered as a function  $I : E \rightarrow \mathbb{Z}$  (with  $E = [0, 511]^3$ ), associating to each point  $x \in E$  its gray-level  $I(x)$  in the image. Since the method is fully automatic, no other parameter is required. It provides as output a binary image  $S \subset E$  corresponding to the segmented coronary arteries visualised in  $I$ .

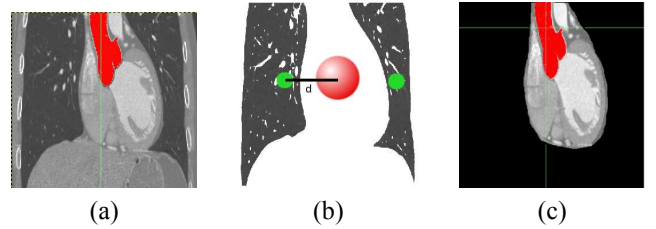


**Fig. 3.** (a) Original image, (b) Structuring element used for the heart zone detection and (c) heart zone detected.

### 3.2. Heart zone detection

As described above, the image  $I$  has huge dimensions, while the coronary arteries which have to be segmented from it are small structures. Consequently, their segmentation from  $I$  without any preprocessing step will necessarily results in a prohibitive computational cost. In order to reduce this cost, two strategies can be considered: 1) working on a subsampled image of  $I$  whenever it is possible, and 2) reducing the region of  $I$  where the coronary arteries are supposed to be localised.

Until starting the actual segmentation of the coronary arteries (Section 3.3.2), all the steps of the method (which do not require a fine resolution of the image) can be performed on a subresolution version  $I_s$  of  $I$ . This image  $I_s : E_s \rightarrow \mathbb{Z}$  is defined by  $I_s(x) = \min\{I(y) \mid y \in 4x + [0, 3]^3\}$  is an approximation of  $I$  where the high intensity small details have been removed.

The computational cost reduction induced by this subsampling can be optimised by also determining a region of interest of  $I_s$  where will be located the vascular structures, namely the heart region. The idea is then to use a GL HMT considering

the lungs as background and the heart as object. The heart zone detection is realized with two *ad hoc* structuring elements: a sphere for  $A$ , and for  $B$  one of two spheres, smaller than  $A$  and whose centers are horizontally symmetrical w.r.t. the center of  $A$  (Fig. 3(b)). After study of a representative number of images, we have an average of difference of intensity in the order of a value 200. The GL HMT (Eq. 2) result in a subset  $S_s^h \subset E_s = [0, 127]^3$  which corresponds to the heart region (Fig. 3(c)).

### 3.3. Coronary arteries detection

A naive way to segment coronary arteries could be a straightforward application of GL HMT using structuring elements modelling the tubular structures and their background. This would discern not only the coronary arteries, but also other vessels of the heart, such as the coronary veins which are close to coronary arteries (Fig. 1(a)). In order to avoid such problems and to efficiently perform segmentation, a solution, described in the sequel, consists in taking advantage of *a priori* anatomic knowledge related to the coronary arteries, in particular their size, their position (near the heart surface), and their initial point (on the aorta), to design a segmentation strategy in adequation with this knowledge.

#### 3.3.1. Aorta automatic detection

About 2 to 3 cm above the aortic valve, an axial section of the aorta presents a circular shape (Fig. 4), with a radius varying from 1 cm to 2 cm, this value depending on the patient and the conditions of the image acquisition. Starting from the obtained subset  $S_s^h$  we create a new subset  $S_s^a$  representing the aorta. Our goal is to localize this circular shape using a GL HMT with multi-sized structuring elements. A horizontal disk ( $A$ ) with a variable radius models the object. To model the background, we surround this disk with 8 points regularly sampled on a discrete circle presenting ( $B$ ) (Fig. 5(a)).

It is easy to notice that the dark space where the background of the structuring element should fit is relatively fine, an image erosion would thus allow to widen this region. Once this circular shape is detected, we calculate the medium value of intensity on this cut. The center of the detected circular shape will be used as seed for a first region-growing, the expansion criterion of which will involve two parameters: intensity thresholding and variance [10]. This region-growing will be stopped by the aorta wall on the sides and by the aortic valve down (Fig. 5(b)). The GL HMT (Eq. 2) followed by the region-growing results in the subset  $S_s^a \subset E_s^a$  which corresponds to the aorta segment.

#### 3.3.2. Coronary arteries seed point detection

The coronary arteries are the only tubular structures that arise from the aorta. The idea is to search them in the wall of the aorta. Starting to search a thinner and a smaller object, we need a high definition, a comeback to the original size becomes necessary. We realise an over-sampling of the aorta to

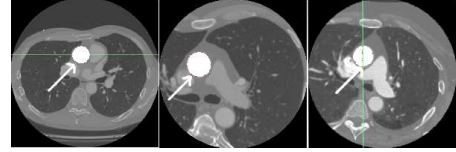


Fig. 4. Examples of the aorta horizontal axial-section.

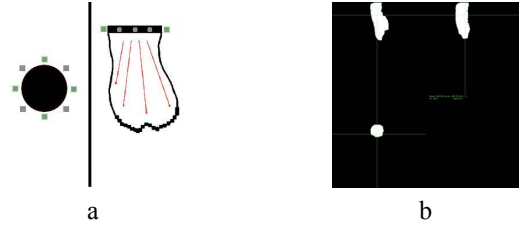


Fig. 5. Aorta detection: (a) structuring element for the circular axial-section detection and (b) the segmented aorta.

go back to the original size ( $512^3$ ). A over-sampled version  $S^a$  of  $S_s^a$  is then obtained as  $S^a = \cup_{x \in E} (4.x + [0, 3]^3)$ .

Following a strategy close to the one proposed in [11], a GL HMT is applied, with a sphere as object and 4 points surrounding this sphere as background. These points belong to the plane normal to the artery axis. The choice of these points defines the axis direction of the searched coronary artery. 13 structuring elements, corresponding to the 13 discrete principal directions are then used (Fig. 6(a)).

This GL HMT is applied on the aorta wall, thus we obtain two seed points  $S_l = (x_l, y_l, z_l)$  and  $S_r = (x_r, y_r, z_r) \in S^a$  for the left and right artery coronaries.

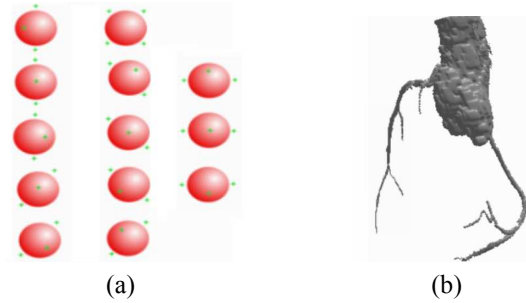


Fig. 6. (a) Structuring element used for the coronary arteries detection and (b) detected coronary arteries.

#### 3.3.3. Region-growing for coronary arteries detection

Starting from the two seed-points  $S_r$  and  $S_l$  previously detected on the aorta wall, a region-growing is performed, applying the GL HMT on every neighbour as criterion. The involved structuring elements are the same as those described in the previous subsection for the seed-points detection. The result is a subset  $S \subset E$  which corresponds to the coronary

arteries. An example of result (aorta and coronary arteries) is illustrated in Fig. 6(b).

#### 4. EXPERIMENTS AND RESULTS

As a first step of validation, this method was tested on 4 coron-scan images, visually providing satisfactory results. In a second step the validation on a base of 40 images was realised. Because of the changeability of processed images, some modifications were added in order to make more uniform the variations between the different images, especially the contrast which is critical in the application of the GL HMT. Then a preprocessing is applied on the heart zone image  $S^h \subset E$ , an erosion followed by an under-sampling keeping only the minimum of intensities is applied to acquire a first image  $I_{se}^h \subset E_s$ , followed by an over-sampling to get a new  $512^3$  image  $I_e^h \subset E$ . At the same time, and on  $I^h$ , a dilation followed by an under-sampling keeping only the maximum of intensity is applied to acquire a first image  $I_{sd}^h \subset E_s$ , followed by an over-sampling to get a new  $512^3$  image  $I_d^h \subset E$ . Then a variant of the GL HMT is considered, we apply this new GL HMT with the object structuring element in  $I_d^h$  and the background structuring element in  $I_e^h$ . We call it a soft GL HMT in reference to the soft morphological filters that use similar modifications. We had satisfactory results on 95% of our base. In this method, some dimensions had to be set, like the radius of the horizontal disk in the aorta detection. The user does not have to fix these measurements, but they are constants in the algorithm which present an average calculated on the whole image base, with a standard deviation set through all the base. As results we got a large part of the coronary arteries, however some small bifurcations were not detected, due to the fall of the contrast between these segments and their background.

##### 4.1. Final algorithm

Input: Original image:  $I : E \rightarrow \mathbb{Z}$  with  $512^3$  size.

- Under-sampling to get a  $128^3$  image:  
 $I_s(x) = \min\{I(y) \mid y \in 4.x + [0, 3]^3\}$ .
- Heart zone detection by GL HMT application:  $S_s^h \subset E_s$ .
- Over-sampling to get a  $512^3$  image:  $S^h \subset E$ .
- Coronary arteries detection.
  - Aorta segmentation:  $S_s^a \subset E$ .
    - \*  $S^h$ - erosion :  $I_e^h \subset E$
    - \* Under-sampling  $I_e^h$  to get a  $128^3$  image:  
 $I_{se}(x) = \min\{I(y) \mid y \in 4.x + [0, 3]^3\}$ .
    - \* Over-sampling to get a  $512^3$  image:  $I_e(x)$ .
    - \*  $S^h$ - dilation :  $I_d^h \subset E$
    - \* Under-sampling to get a  $128^3$  image:  
 $I_{sd}(x) = \max\{I(y) \mid y \in 4.x + [0, 3]^3\}$ .
    - \* Over-sampling to get a  $512^3$  image:  $I_d(x)$ .
    - \* Circular coron-section localisation, using  $I_e(x)$  and  $I_d(x)$  at the same time.
    - \* Calculate the medium intensity on this coron-section.
    - \* Region-growing starting by the circular shape center and using the calculates medium intensity as criterion.
  - Search of the two coronary arteries seed points on the aorta wall:  $S_r$  and  $S_l$ .
  - Artery coronaries detection with a region-growing using GL HMT as criterion:  $S \subset E$ .

Output: Coronary arteries  $512^3$  image:  $I^c$ .

#### 5. CONCLUSION AND FUTURE WORK

Improvements are being implemented, as in the detection of the aorta, it shall be probably more competitive to accomplish the region-growing with a GL HMT more efficient than a criterion of intensity and its variation, using the same structuring element as the one used to detect the circular shape in a non-rigid version. Other improvements are under way of realization, such as the progressive and adaptive region-growing in the coronary arteries. Based on the knowledge that as far as we go in the coronary arteries, the contrast between them and their background, as well as their size, decrease, we set a progressive GL HMT to make the region-growing, and to go farther and to the smallest forks of the coronary arteries.

Once these new improvements are definitely validated, a study will be undertaken on the behaviour of the coronary arteries in the 4<sup>th</sup> dimension: time. In order to realize this study, we have to adapt this method to the 4<sup>th</sup> dimension, independently from the data changes from a phase to the next one.

#### 6. REFERENCES

- [1] C. O'Callaghan et al., *Stress and the Heart: Psychosocial Pathways to Coronary Heart Disease*, Wiley, 2002.
- [2] C. Blondel, R. Vaillant, F. Devernay, G. Malandain, and N. Ayache, "Automatic trinocular 3D reconstruction of coronary artery centerlines from rotational X-ray angiography," in *Computer Assisted Radiology and Surgery 2002, Proceedings*, 2002, pp. 1073–1078, Springer.
- [3] J.S. Suri, K. Liu, L. Reden, and S. Laxminarayan, "A review on MR vascular image processing: Skeleton versus nonskeleton approaches: Part II," *IEEE Transactions on Information Technology in Biomedicine*, vol. 6, no. 4, pp. 338–350, 2002.
- [4] C. Kirbas and F. Quek, "A review of vessel extraction techniques and algorithms," *ACM Computing Surveys*, vol. 36, no. 2, pp. 81–121, 2004.
- [5] B. Bouraoui, C. Ronse, J. Baruthio, N. Passat, and Ph. Germain, "Gray-level hit-or-miss transform based region-growing for automatic segmentation of 3D coronary arteries," in *International Symposium on Mathematical Morphology 2007, Proceedings*, 2007, vol. 2, pp. 23–24.
- [6] C. Lorenz, S. Renisch, T. Schlatholter, and T. Bulow, "Simultaneous segmentation and tree reconstruction of the coronary arteries in MSCT images," *SPIE Medical Imaging: Physiology and Function: Methods, Systems, and Applications 2003, Proceedings*, vol. 5031, pp. 167–177, 2003.
- [7] N. Passat, C. Ronse, J. Baruthio, J.-P. Armspach, C. Maillot, and C. Jahn, "Region-growing segmentation of brain vessels: An atlas-based automatic approach," *Journal of Magnetic Resonance Imaging*, vol. 21, no. 6, pp. 715–725, 2005.
- [8] P. Soille, *Morphological Image Analysis*, Springer-Verlag, Heidelberg, 2nd edition, 2003.
- [9] B. Naegel, N. Passat, and C. Ronse, "Grey-level hit-or-miss transforms - Part II: Application to angiographic image processing," *Pattern Recognition*, vol. 40, no. 2, pp. 648–658, 2007.
- [10] J. Fleureau, M. Garreau, A.I. Hernández, A. Simon, and D. Boulmier, "Multi-object and N-D segmentation of cardiac MSCT data using SVM classifiers and connectivity algorithm," in *Computers in Cardiology 2006, Proceedings*, 2006, vol. 33, pp. 817–820.
- [11] B. Naegel, C. Ronse, and L. Soler, "Using grey-scale hit-or-miss transform for segmenting the portal network of the liver," in *Mathematical Morphology: 40 years on. Proceedings of the 7th International Symposium on Mathematical Morphology*, C. Ronse, L. Najman, and E. Decencière, Eds., Paris, France, April 2005, vol. 30 of *Computational Imaging and Vision*, pp. 429–440, Springer SBM.